

---

# INCORPORATING PRE-TRAINING DATA MATTERS IN UNSUPERVISED DOMAIN ADAPTATION

---

A PREPRINT

Yinsong Xu<sup>1,3</sup>, Aidong Men<sup>1</sup>, Yang Liu<sup>2</sup>, Qingchao Chen<sup>3,†\*</sup>

<sup>1</sup>Beijing University of Posts and Telecommunications

<sup>2</sup>Wangxuan Institute of Computer Technology, Peking University

<sup>3</sup>National Institute of Health Data Science, Peking University

August 8, 2023

## ABSTRACT

Unsupervised domain adaptation(UDA) and Source-free UDA(SFUDA) methods formulate the problem involving two domains: source and target. They typically employ a standard training approach that begins with models pre-trained on large-scale datasets *e.g.*, ImageNet, while rarely discussing its effect. Recognizing this gap, we investigate the following research questions: (1) *What is the correlation among ImageNet, the source, and the target domain?* (2) *How does pre-training on ImageNet influence the target risk?* To answer the first question, we empirically observed an interesting *Spontaneous Pulling (SP) Effect* in fine-tuning where the discrepancies between any two of the three domains (ImageNet, Source, Target) decrease but at the cost of the impaired semantic structure of the pre-train domain. For the second question, we put forward a theory to explain SP and quantify that the target risk is bound by gradient disparities among the three domains. Our observations reveal a key limitation of existing methods: it hinders the adaptation performance if the semantic cluster structure of the pre-train dataset (i.e. ImageNet) is impaired. To address it, we incorporate ImageNet as the third domain and redefine the UDA/SFUDA as a three-player game. Specifically, inspired by the theory and empirical findings, we present a novel framework termed **TriDA** which additionally preserves the semantic structure of the pre-train dataset during fine-tuning. Experimental results demonstrate that it achieves state-of-the-art performance across various UDA and SFUDA benchmarks.

## 1 Introduction

It is well-known that deep learning models are susceptible to failure when the test data (target domain) differs significantly from the training data (source domain) [8, 35]. This problem referred to as domain shift, is addressed by Unsupervised Domain Adaptation (UDA) via knowledge transfer [43, 22, 3]. The objective of UDA is to enhance the performance on an unlabeled target domain by harnessing the labeled data from the source domain.

Existing methods formulate UDA as a problem composed of two domains: source and target. The seminal domain adaptation theory [2] bounds the target risk with the source risk, domain discrepancy, and an ignorable constant. This theory has profoundly inspired UDA methods, which endeavor to concurrently minimize the source classification loss and align the source and target distribution via *i.e.*, domain-adversarial methods [6, 24] and discrepancy measurement [52]. Recently, source-free UDA (SFUDA) is introduced where source data is inaccessible during adaptation on the target domain due to considerations related to privacy or intellectual property. Existing SFUDA works turn to cluster [20, 48] and pseudo-labels methods [17] for supervision.

Existing deep learning UDA methods typically employ a training approach that initiates from models pre-trained on extensive datasets such as ImageNet [4]. Empirical evidence has shown that pre-training on ImageNet enhances performance and speeds up convergence, particularly when the target dataset is small [9]. [36] provide generalization

---

\*† Qingchao Chen is the corresponding author

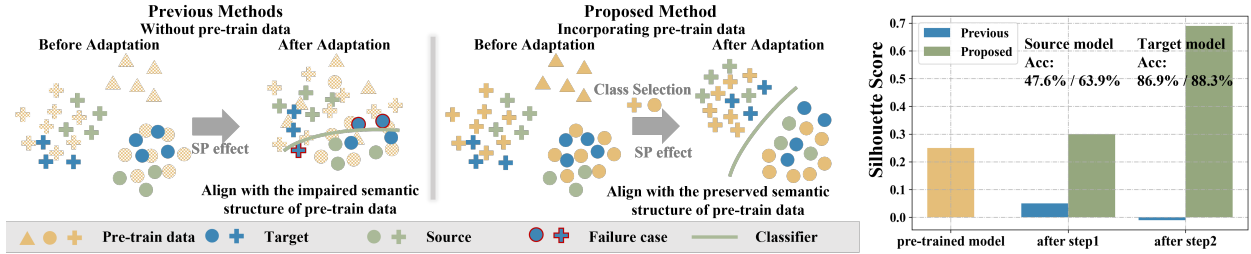


Figure 1: (Best viewed in color) Comparison of previous and proposed methods. **Left:** Previous methods do not consider the pre-train data and its impaired semantic structure. **Middle:** Our method incorporates pre-train data into training. **Right:** Our method preserves the semantic structure of pre-train data and improve the performance.

bounds with general losses, tasks, and features. However, it is important to note that the benefits may not always be realized, especially when the target dataset bears little resemblance to ImageNet [30]. Despite these observations, the influence of pre-training on UDA performance has rarely been examined in previous studies. Acknowledging this gap, we aim to address the following research questions: (1) *What is the relation among ImageNet, the source, and the target domain?* (2) *How does pre-training on ImageNet affect the target risk?*

To answer the two questions, we conduct both empirical and theoretical analyses. **For the first question,** we explore the domain correlation by measuring the domain discrepancy throughout the adaptation process. We empirically observed an interesting *Spontaneous Pulling (SP) Effect* and related three characteristics. (1)*The discrepancies between any two of the three domains (ImageNet, Source, Target) decrease during fine-tuning.* (2)*The label noise is an essential factor to determine the SP Effect.* (3)*The semantic structure of ImageNet is impaired during fine-tuning.* **For the second question,** we put forward theoretical implications, explaining and quantifying the SP Effect and how pre-training (i.e. ImageNet) influences the target risk through the lens of model optimization with stochastic gradient descent. The key idea is that when confronted with a dataset with limited sample size, the target risk is bound by the model gradient disparities between the target and the source domain, as well as that between the target domain and the pre-train data.

Our observation and theory reveal a key limitation of existing methods, as shown in the left side of Figure 1. They fail to preserve the cluster structure of the pre-train dataset and ignore the SP Effect (details in 5.3). The SP Effect and the impaired semantic structure of the pre-train dataset hinder the target domain adaptation and increase the risk of negative transfer(details in 5.3).

Inspired by the SP Effect and its theoretical implications, we propose to boost the adaptation performance by *decreasing* the cross-domain discrepancy and *maintaining the semantic structures* of the pre-train dataset simultaneously. To achieve it, we perceive the pre-train dataset (ImageNet) as a third domain in addition to the source and target domains, redefining UDA as a three-player game. We introduce a novel framework, referred to as TriDA, to enhance target performance in both UDA and SFUDA. *Specifically,* we propose to reduce the cross-domain gradient disparities within the feature embedding and classifier boundaries meanwhile preserving the semantic structures of the pre-train dataset. In addition, we propose a novel and efficient strategy to select relevant pre-train data based on semantic similarities. We make the following contributions in this work:

- We introduce the *Spontaneous Pulling (SP) Effect* elucidating the correlation among pre-train data, the source, and target domains. We put forward a theory to exhibit the effect on pre-train data during adaptation.
- This paper redefines UDA as a three-player game among the source, target, and ImageNet domains, and proposes TriDA which boosts the adaptation performance by additionally preserving semantic structure of pre-train data.
- The proposed method is evaluated on multiple benchmarks in both vanilla UDA and SFUDA scenarios, demonstrating SOTA performance.

## 2 Related Work

### 2.1 Pre-training and Fine-tuning

The "pre-training → fine-tuning" paradigm, also known as transfer learning, has been the *de facto* choice for deep learning. It achieves state-of-the-art results in many computer vision applications [19, 27] thanks to large-scale datasets [4, 45] and public pre-trained models offered by PyTorch, TensorFlow, and third-party libraries. In spite of the immense popularity, some recent works argue the paradigm. [10] shows that ImageNet pre-training brings fewer benefits for the

localization task compared with classification. [15] illustrates that learned features from ImageNet do not transfer well to fine-grained classification tasks.

A group of works focuses on how to better utilize the pre-trained knowledge from the source dataset [44, 40, 1]. Co-tuning [50] retains the task-specific parameters and learns the relationship among categories. [23] boosts the performance by incorporating a subset of pre-train data into fine-tuning.

## 2.2 Vanilla Unsupervised Domain Adaptation

In vanilla UDA, we have access to a labeled source and an unlabeled target dataset. Adversarial learning based methods [7] use a feature generator and a domain discriminator that play a minimax game to align the marginal [6] or conditional distribution [24]. [18] encourages the bi-classifier to generate disagreement prediction to improve target features' categorical discriminability. [21] generates pseudo labels with class centroids. Another group works propose distribution discrepancy measurements to promote domain confusion in the feature space, *e.g.*,  $\mathcal{H}\Delta\mathcal{H}$ -divergence [2], Maximum Classifier Discrepancy [32] and Maximum Mean Discrepancy [34]. [52] proposes a novel measurement, Margin Disparity Discrepancy, based on the scoring functions and margin loss. [26] points out that mixup [51] helps knowledge transfer gradually from the source to the target domain.

## 2.3 Source-free Unsupervised Domain Adaptation

In SFUDA [20, 5, 28], only the unlabeled target data and the model pre-trained by source data are available during adaptation. Pseudo-labeling is the mainstream framework adopted by a group of works [20, 17]. For instance, SHOT [20] generates pseudo labels via clustering and uses information maximization and entropy minimization. CoWA [17] generates pseudo labels from Gaussian Mixture Modeling. Due to the unavailability of the source domain in the adaptation, direct minimization of the domain discrepancy becomes infeasible. To address it, [5] treats the classifier weights as centers of source features and then minimizes the discrepancy between the surrogate source and target distribution. DaC [53] identifies source-like samples via class clustering and aligns the two domains using a memory-based Maximum Mean Discrepancy. Additionally, the local neighbor structure is applied to provide effective supervision for model optimization [49, 47]. Besides, [16] demonstrates that image- and feature-mixup is beneficial to the discriminability-transferability tradeoff.

In this paper, we introduce TriDA, a novel framework that integrates pre-train into the adaptation. This framework redefines domain adaptation as a three-player game, thereby showing uniqueness from existing methods that consider only the source and target domains. TriDA can be applied in both vanilla UDA and SFUDA, demonstrating superior performance in our experiment section.

# 3 The Role of Pre-train Dataset in UDA

## 3.1 Preliminaries

In unsupervised domain adaptation (UDA), we are given a labeled source set,  $\mathcal{D}_S = \{(x_S^i, y_S^i)\}_{i=1}^{n_S}$ , drawn from the distribution  $P_S$  and an unlabeled target set,  $\mathcal{D}_T = \{x_T^i\}_{i=1}^{n_T}$ , drawn from the distribution  $P_T$ , where  $x \in \mathcal{X}$  is the input space,  $y \in \mathcal{Y}$  is the label space. The aim of UDA is to learn a hypothesis,  $h : \mathcal{X} \rightarrow \mathcal{Y}$ , to predict the labels in  $\mathcal{D}_T$ , and the risk is given by  $\epsilon_T(h) = \mathbb{E}_{x \sim P_T} \mathbb{1}[h(x) \neq y]$ , where  $\mathbb{1}[\cdot]$  is the indicator function. The seminal work [2] gives a bound on  $\epsilon_T(h)$  in the following:  $\epsilon_T(h) \leq \epsilon_S(h) + \frac{1}{2}d_{\mathcal{H}\Delta\mathcal{H}}(P_S, P_T) + \lambda$ , where  $d_{\mathcal{H}\Delta\mathcal{H}}(\cdot, \cdot)$  is the  $\mathcal{H}\Delta\mathcal{H}$ -divergence, and  $\lambda = \epsilon_T(h^*) + \epsilon_S(h^*)$  is the combined risk, and  $h^* = \arg \min_{h \in \mathcal{H}} \epsilon_T(h) + \epsilon_S(h)$ .

Inspired by it, most vanilla UDA [6, 24, 18] and SFUDA [20, 17, 49, 47] methods propose to use the source loss (*e.g.*, cross-entropy) and the domain alignment loss (*e.g.*, adversarial loss, pseudo label loss) to lower the first two items on the RHS of the bound, either simultaneously (UDA) or step-wise (SFUDA). Serving as the initialization of models and the key factors of the hypothesis space, the pre-trained weight plays an extremely essential role in the UDA. *However*, the analysis of the pre-train data and its pre-trained models received very limited attention, motivating further investigations into its effects in our submission.

## 3.2 The Spontaneous Pulling Effect

In this section, we explore the relationships among pre-train data, the source, and the target domains via domain discrepancy during the adaptation process. We consider pre-train data as the third domain, which is denoted as  $\mathcal{D}_I = \{(x_I^i, y_I^i)\}_{i=1}^{n_I}$  drawn from the distribution  $P_I$ . We analyze the Wasserstein distance (w-distance for abbreviation), a domain discrepancy measurement in UDA [33, 14], which measures the divergence of the feature-level marginal

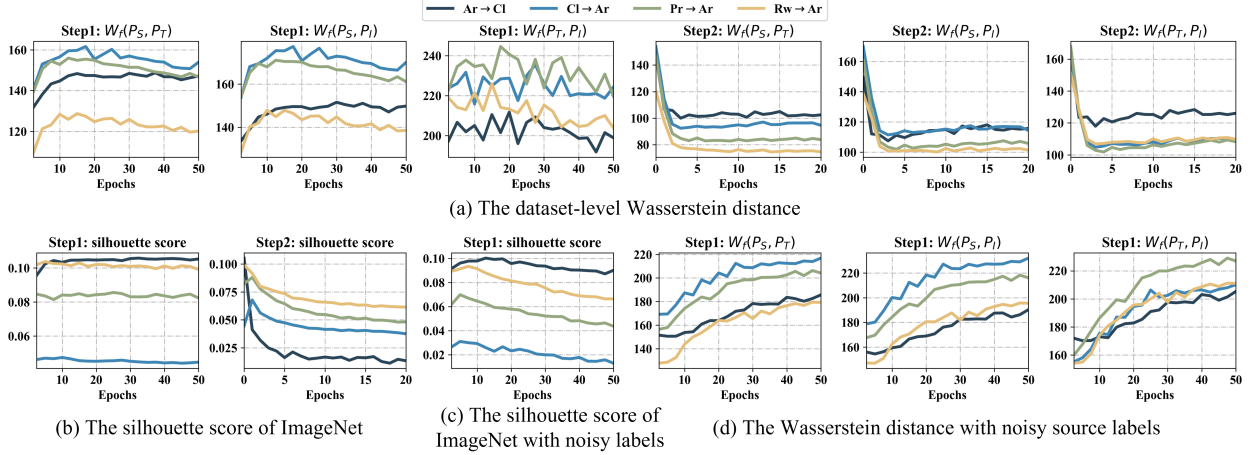


Figure 2: The trends of the Wasserstein distance during training. (a) It represents a spontaneous decrease among the three domains. (b) The decline of the silhouette score indicates that the clustering semantic structures of ImageNet are broken. (c) Noisy labels speed up the decrease of silhouette scores. (d) Discrepancies increase with noisy labels.

distribution:

$$W_f(P, P') = \inf_{\gamma \in \Pi(P, P')} \mathbb{E}_{(x, x') \sim \gamma} \|f(x) - f(x')\|, \quad (1)$$

where  $\Pi(P, P')$  denotes the set of all joint distributions  $\gamma(x, x')$ , and  $f(\cdot)$  denotes feature embedding. We also propose to assess the semantic structure of the pre-train dataset (ImageNet) using the silhouette score (a metric that quantifies intra-cluster consistency) of the features.

We evaluate *SHOT* [20] as a representative SFUDA method, and conduct analysis on Office-Home[38]. The training consists of two steps. **Step 1:** fine-tune ImageNet pre-trained model using source data and labels; **Step 2:** fine-tune the step 1 model using target domain data and its pseudo labels.

**Observation 1.** *Fine-tuning using the source data and ground-truth label only, the discrepancies between any two of the three domains (ImageNet, Source, Target) decrease.*

In Figure 2(a), We notice the w-distance ascent in the early epochs of step 1, which may be due to the randomly initialized bottleneck and classifier modules. Subsequently, the w-distance decreases, though the target domain does not participate in step 1 training. Similarly in step 2, we witness a significant reduction in the early training period. We term it as the *Spontaneous Pulling (SP) Effect* among the domains in UDA because we did not use any explicit loss to reduce the discrepancies and it happens almost *spontaneously*.

**Observation 2.** *The label noise in the fine-tuning is an essential factor to determine SP Effects, i.e., the domain discrepancies among the three.*

(1) We fix other factors and re-train the model by adding noise to source labels, where 50% of the labels were replaced by random ones. The re-trained results are depicted in Figure 2(d), where an *obviously increased discrepancy* is observed in contrast with the trend in Figure 2. (2) It also suggests that the slight increase of  $W_f(P_T, P_I)$  in final epochs in Figure 2(a) is attributable to the noisy target pseudo-labels in step 2.

**Observation 3.** *The concurrent decrease of the silhouette score in pre-train data is observed with the SP Effect in the fine-tuning. The silhouette score of pre-train data decreases by a larger margin when fine-tuning using the noisy label, compared with using the ground-truth labels.*

(1) As depicted in Figure 2(b), the silhouette scores of ImageNet features decline whether the model is fine-tuned using ground-truth source domain labels (step 1) or pseudo-labels in the target domain (step 2). It indicates that the clustering semantic structures of ImageNet are broken. (2) We plot the silhouette score of ImageNet features with noisy source labels in Figure 2(c). It shows that incorrect labels speed up the decrease, which also accounts for the faster decrease in Figure 2 due to the noisy target pseudo-labels (b) in step 2.

The above observations summarize the correlation among pre-train data (*i.e.*, ImageNet), the source, and the target domain and more importantly, infer the following arguments related to SP effects: (1) in the fine-tuning stage, source domain semantic structures are improved (increased silhouette) while inevitably impairing the one of pre-train data (decreased silhouette). (2) without any explicit loss to pull the source domain and pre-train data closer in the fine-tuning

stage, although with the impaired semantic structure of pre-train data, the SP Effect still happens, i.e. discrepancies among the three domains still decrease. We ask a question: *will it decrease the discrepancies further and boost the adaptation performance if we maintain the semantic structures in both the pre-train data and the source/target domain simultaneously?* It also reveals a key gap in existing UDA methods: they use the ImageNet pre-trained models as the starting point of the adaptation but ignore to analyze its effects and the SP Effect.

### 3.3 Theoretical Implications

We present theoretical implications to show the effect of the pre-train dataset (ImageNet) on the adaptation performances of the target domain and the SP Effect. Details can be found in Supplementary.

**Notation.** We denote the optimization problem as  $\min_{\theta} \mathcal{L}(\theta) := \mathbb{E}_{(x,y) \in \mathcal{P}} \ell(\theta; x, y)$ .  $\theta \in \mathbb{R}^d$  is the model parameters updated by SGD:  $\theta_{t+1} = \theta_t - \eta \nabla \ell(\theta_t; x_{it}, y_{it})$ , where  $t = 0 : T$  indicates the iteration index, and  $\eta$  is the learning rate. For the sake of the analysis, it is assumed that all domains share the same set of parameters. We measure the model’s performance with excess risk. Denote the excess risk of pre-trained model as  $\tilde{\mathcal{L}}(\theta) = \mathcal{L}(\theta) - \mathcal{L}(\theta^*)$ , where  $\theta^* \in \arg \min_{\theta \in \mathbb{R}^d}$  is the optimal solution. The subscript of  $\mathcal{L}/\tilde{\mathcal{L}}$  indicates the domain where the expectation is computed, while the subscript of  $\theta$ ,  $T$ , and  $\eta$  indicates the domain where the model is trained.

**Proposition 1.** (Source-only) *Denote the ImageNet pre-training and source training corresponding to subscript  $I$ ,  $S$ , respectively. There exists a constant  $\mu > 0$  such that:*

$$\tilde{\mathcal{L}}_T(\theta_I) \leq \frac{\Delta_I^2}{\mu}, \text{ where } \|\nabla \mathcal{L}_I(\theta) - \nabla \mathcal{L}_T(\theta)\| \leq \Delta_I. \quad (2)$$

$$\tilde{\mathcal{L}}_T(\theta_S) \leq \exp(-\eta_S \mu T_S) \frac{\Delta_I^2}{\mu} + \frac{\Delta_S^2}{\mu}, \text{ where } \|\nabla \mathcal{L}_S(\theta) - \nabla \mathcal{L}_T(\theta)\| \leq \Delta_S. \quad (3)$$

Proposition 1 implies that the performance of the source-only model  $\theta_S$  is bounded by  $\Delta_I$  and  $\Delta_S$ .  $\Delta_I$  represents the gradient differences calculated between the pre-train and the labeled target samples. The same as  $\Delta_S$ . Next, we show how the pre-train dataset (ImageNet) affects the model after adaptation.

**Proposition 2.**(UDA) *Suppose  $\mathcal{L}_{\gamma}(\theta) := \mathbb{E}_{(x_S, y_S, x_T) \in \gamma} \ell_{\gamma}(\theta; x_S, y_S, x_T)$  is the proposed objective function during training jointly on the source and target domain. There exists a constant  $\mu > 0$  such that:  $\tilde{\mathcal{L}}_T(\theta_T) \leq \exp(-\eta_{\gamma} \mu T_{\gamma}) \frac{\Delta_I^2}{\mu} + \frac{\Delta_{\gamma}^2}{\mu}$ , where  $\|\nabla \mathcal{L}_{\gamma}(\theta) - \nabla \mathcal{L}_T(\theta)\| \leq \Delta_{\gamma}$ .*

**Proposition 3.**(SFUDA) *Suppose  $\mathcal{L}'_T(\theta) := \mathbb{E}_{(x,y) \in P_T} \ell'(\theta; x)$  is the proposed objective function during adaptation on the unlabeled target domain. There exists a constant  $\mu > 0$  such that:  $\tilde{\mathcal{L}}_T(\theta_T) \leq \exp(-\eta_T \mu T_T) \tilde{\mathcal{L}}_T(\theta_S) + \frac{\Delta_T^2}{\mu}$ , where  $\|\nabla \mathcal{L}'_T(\theta) - \nabla \mathcal{L}_T(\theta)\| \leq \Delta_T$ .*

Propositions 2 and 3 imply that the adaptation performance of UDA and SFUDA is bounded by  $\Delta_{\gamma}$  and  $\Delta_T$  respectively.  $\Delta_T$  describes the gradient difference between using the objective with ground-truth supervision and the one using the proposed unsupervised alternatives i.e., the accuracy of pseudo-labels, while  $\Delta_{\gamma}$  depicts the gradient disparity when employing the UDA objective, i.e., the domain discrepancy and source risk.

Theoretical considerations suggest that the adaptation performance is influenced by gradient disparities, i.e.,  $\Delta$ . It offers an explanation for the impaired semantic structure of pre-train data in the SP Effects. The number of iterations,  $T_S$  and  $T_T$ , is correlated with the dataset size of the source and target domain. Thus, the effect of pre-train data is insignificant when we have enough source and target samples.

## 4 Method

These theoretical insights motivate us to incorporate pre-train data into the training process. We unify pre-train into the framework and redefine UDA/SFUDA as a three-player game, thereby deviating from conventional methods that only consider the source and the target domains. As a result, we introduce our proposed framework, referred to as TriDA, as illustrated in Figure 3. The three domains share the feature extractor  $f$ . We denote the features as  $v = f(x)$ , the source/target classifier as  $c$ . Additionally, we incorporate a pre-train data classifier  $c_I$ , which can be removed after training, thereby enhancing the adaptation performance without incurring additional inference costs.

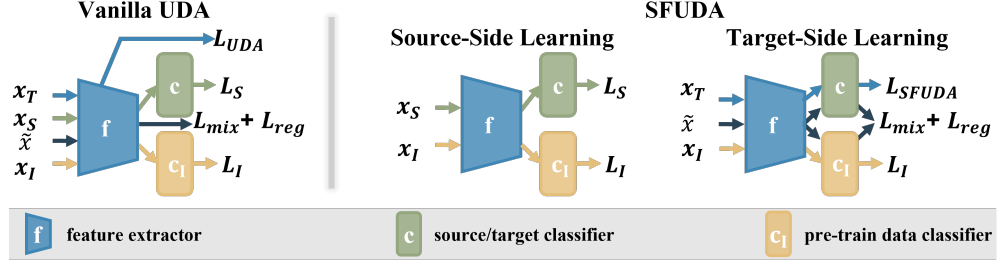


Figure 3: Training pipeline of TriDA .

#### 4.1 TriDA Framework

**Source-Side Learning.** In this step, our goal is to learn a model on the labeled source domain, which serves as the initialization for the target model. Initially, we adhere to the standard DA practice of reducing the source risk  $\mathcal{L}_S$ . Additionally, we introduce  $\mathcal{L}_I$  to preserve the cluster structure of pre-train data. Thus, the overall objective function is formulated as:

$$\min_{f, c, c_I} \mathcal{L}_S + \beta_I \mathcal{L}_I, \quad (4)$$

where  $\mathcal{L}_S = \mathbb{E}_{(x_S, y_S) \in P_S} \ell_{ce}(c(v_S), y_S)$ , and  $\mathcal{L}_I = \mathbb{E}_{(x_I, y_I) \in P_I} \ell_{ce}(c_I(v_I), y_I)$ , and  $\ell_{ce}$  is cross-entropy and  $\beta_I$  is the trade-off parameter.

**Target-Side Learning.** Recent UDA works [41, 46, 26] utilize mixup between source and target samples, bridging the two domains. However, this approach is impractical in SFUDA, as source and target data are not concurrently available. Guided by theoretical considerations and acknowledging the different label spaces, we implement an asymmetric mixup to minimize gradient disparities in two areas: classification boundaries and feature embedding. Firstly, we linearly interpolate target images  $x_T$  and ImageNet images  $x_I$  to generate mixup images  $\tilde{x} = \lambda x_T + (1 - \lambda)x_I$ , where  $\lambda \sim \text{Beta}(\alpha, \alpha)$  is the mixup ratio. Predictions for  $\tilde{x}$  are then generated in two label spaces by  $c$  and  $c_I$ . We utilize a weighted sum of the cross-entropy as the loss function, denoted as  $\mathcal{L}_{mix}$ . This supervises the images from two label spaces to minimize gradient disparities in classifier boundaries. The loss function is formulated as follows:

$$\mathcal{L}_{mix} = \mathbb{E}_{(x_I, y_I) \in P_I} \mathbb{E}_{(x_T, \hat{y}_T) \in P_T} \lambda \ell_{ce}(c_I(\tilde{v}), y_I) + (1 - \lambda) \ell_{ce}(c(\tilde{v}), \hat{y}_T), \quad (5)$$

where  $\hat{y}_T$  is the pseudo-label of the target domain generated by the UDA/SFUDA method that we plug our method in.

For feature embedding, we introduce a regularization loss  $\mathcal{L}_{reg}$  that drives the feature  $\tilde{v}$  of  $\tilde{x}$  closer to the mixed feature:

$$\mathcal{L}_{reg} = \mathbb{E}_{(x_I, y_I) \in P_I} \mathbb{E}_{(x_T, y_T) \in P_T} \|\lambda v_I + (1 - \lambda)v_T - \tilde{v}\|_1. \quad (6)$$

It serves as a regularizer to minimize gradient disparities in the feature embedding. Furthermore, mixup facilitates the transfer of information from pre-train to the unlabelled target domain, thus providing additional supervision and constraints. In summary, the objective function in SFUDA is as follows:

$$\min_{f, c, c_I} \mathcal{L}_{SFUDA} + \beta_I \mathcal{L}_I + \beta_M (\mathcal{L}_{mix} + \mathcal{L}_{reg}). \quad (7)$$

Our method is plug-and-play, so  $\mathcal{L}_{SFUDA}$  can any existing method,  $\beta_I$  and  $\beta_M$  are trade-off parameters. It can also be utilized in UDA methods whose objective is  $\mathcal{L}_{UDA}$ , and the overall objective function is:

$$\min_{f, c, c_I} \mathcal{L}_S + \mathcal{L}_{UDA} + \beta_I \mathcal{L}_I + \beta_M (\mathcal{L}_{mix} + \mathcal{L}_{reg}). \quad (8)$$

#### 4.2 Incorporating the Pre-train Data

Pre-train data (*i.e.*, ImageNet), comprising tens of millions of images across 1k categories, is significantly larger than any target dataset in the existing UDA benchmark. Consequently, two challenges arise when attempting to incorporate pre-train data into adaptation effectively and efficiently. *Firstly*, the data distribution in pre-train data presents complex multimodal structures, which increases the risk of incorporating unrelated images into the target domain. *Secondly*, the huge gap in dataset scales creates class imbalance during training, *i.e.*, only a few categories from pre-train data are fed into the model in an epoch.

To address the first challenge, we introduce a class-based selection strategy that offers two key advantages: (1) the selection of fewer classes notably decreases the demand for pre-train data, thereby increasing efficiency; and (2) the strategy mitigates the risk from unrelated images. Denote  $C_I = \{C_{I(i)}\}$  and  $C_T = \{C_{T(i)}\}$  as the classes in ImageNet and the target domain, respectively. Owing to differences in the annotation granularity, not all categories in the target

domain are able to be perfectly matched. Thus, we seek to select pre-train samples that are semantically similar because they normally lie closer in the feature space as illustrated in Figure 4.

The selected classes are those exceeding a certain level of semantic similarity to the target classes. The specific semantic similarity is denoted by  $d(C_{I(i)}, C_{T(j)})$  and the selection is performed when the similarity exceeds a threshold  $\tau$ :

$$\hat{C}_I = \{C_{I(i)} \mid \max_j d(C_{I(i)}, C_{T(j)}) > \tau\}. \quad (9)$$

We measure the semantic similarity by determining the shortest path connecting the synset in the WordNet[25] hierarchy tree structure. For instance, ImageNet does not include the category "Telephone" from Office-Home, but the top-2 similar classes are "Pay-phone", "Dial telephone". To address the second challenge, at the beginning of each epoch, we equally draw samples from each class in  $\hat{C}_I$  to form a subset with a similar scale with the target/source domain. This approach empirically ensures class balance during training.

## 5 Experiment

### 5.1 Setup

To verify the effectiveness of TriDA, we evaluate it in a variety of scenarios, including UDA and SFUDA. The code will be released after acceptance.

**Dataset.** **Office-31** [31] is a small-scale DA benchmark that contains 31 object classes of three domains: (Amazon (A), DSLR (D), and Webcam (W)). **Office-Home** [38] is a medium-sized benchmark, consisting of four different domains (Art (Ar), ClipArt (Cl), Product (Pr), and Real-World (Rw)) in 65 categories. **VisDA-C** [29] is a challenging large-scale benchmark for adapting from synthetic to real images. There are a total of 12 categories in each domain.

**Baseline Methods.** For vanilla UDA, we compare TriDA with CDAN [24], MCD [32], and MDD [52]. For SFUDA, we compare with SHOT [20], SFDA [13], A<sup>2</sup>Net [42], NRC [47], HCL [12], DIPE [39], AaD [49], SFDA-DE [5], CoWA-JMDS [17], and DaC [53]. The best accuracy is indicated in bold, and the second-best accuracy is underlined.

**Implementation Details.** We mainly utilize two backbones, ResNet-50 and ResNet-101 [11]. For optimization, we use mini-batch Stochastic Gradient Descent (SGD) with a momentum of 0.9 and a weight decay of 1e-3. The learning rate is set at 1e-3 for backbones pre-trained on ImageNet and 1e-2 for the remaining layers. For all experiments, we maintain the values of  $\beta_I = 0.3$  and  $\beta_M = 0.1$ . Each experiment is performed three times using different random seeds, with the average accuracy being reported. More details can be found in Supplementary.

Table 1: Classification accuracy (%) on Office-31 (ResNet50).

Task	Method	A→D	A→W	D→A	D→W	W→A	W→D	Avg.
UDA	ResNet-50 [11]	79.3	75.8	63.6	95.5	63.8	99.0	79.5
	MCD [32]	87.3	90.4	68.3	98.5	67.6	<b>100.0</b>	85.4
	MDD [52]	94.4	<u>95.6</u>	76.6	98.6	72.2	<b>100.0</b>	89.6
	CDAN [24]	89.9	93.8	73.4	98.5	70.4	<b>100.0</b>	87.7
	Ours+ CDAN	92.2	95.1	75.9	98.5	74.6	<b>100.0</b>	89.4
	SFDA [13]	92.2	91.1	71.0	98.2	71.2	99.5	87.2
SFUDA	A <sup>2</sup> Net [42]	94.5	94.0	<u>76.7</u>	<b>99.2</b>	76.1	<b>100.0</b>	90.1
	NRC [47]	96.0	90.8	75.3	99.0	75.0	<b>100.0</b>	89.4
	HCL [12]	94.7	92.5	75.9	98.2	<b>77.7</b>	<b>100.0</b>	89.8
	DIPE [39]	<b>96.6</b>	93.1	75.5	98.4	77.2	99.6	90.1
	AaD [49]	<u>96.4</u>	92.1	75.0	<u>99.1</u>	76.5	<b>100.0</b>	89.9
	SFDA-DE [5]	96.0	94.2	76.6	98.5	75.5	99.8	90.1
	CoWA[17]	94.4	95.2	76.2	98.5	<u>77.6</u>	99.8	<u>90.3</u>
	TriDA+CoWA	93.6	<b>96.2</b>	<b>77.1</b>	98.6	76.3	<b>100.0</b>	<u>90.3</u>
	SHOT [20]	94.0	90.1	74.7	98.4	74.3	<u>99.9</u>	88.6
	TriDA+SHOT	94.8	94.6	<b>77.1</b>	98.9	76.8	<b>100.0</b>	<b>90.4</b>

Table 2: Ablation study on Office-Home.

Baseline	$\mathcal{L}_I$	$\mathcal{L}_{mix}$	$\mathcal{L}_{reg}$	Avg.
✓				71.8
✓	✓			72.6
✓		✓		72.7
✓	✓	✓		<u>72.8</u>
✓		✓	✓	<u>72.8</u>
✓	✓	✓	✓	<b>72.9</b>

Table 3: Analysis of selected classes

$N_c$	$\tau$	0.0	0.2	0.3	0.4	random
$N_c$	1000	273	146	63	63	
Avg.	72.3	<b>73.2</b>	<u>73.0</u>	72.9	72.6	

### 5.2 Comparison with State-of-the-arts

We evaluate TriDA in both vanilla UDA and SFUDA scenarios on Office-Home, Office-31, and VisDA-C. The results are shown in Tables 1, 4, and 5, respectively. Our method achieves state-of-the-art performance compared to existing methods. Specifically, in UDA, TriDA outperforms the baseline, CDAN, by a large margin (1.7% on Office-31, 1.9% on Office-Home, 2.9% on VisDA-C). In SFUDA, TriDA enhances the baseline, SHOT, by 1.8% on Office-31, 1.1% on Office-Home, and 0.4% on VisDA-C. These results show the efficacy of our method and demonstrate the notion that the integration of ImageNet represents a straightforward yet potent approach to improve vanilla UDA and SFUDA performance.



Table 4: Classification accuracy (%) on Office-Home (ResNet50).

Task	Method	Ar→Cl	Ar→Pr	Ar→Rw	Cl→Ar	Cl→Pr	Cl→Rw	Pr→Ar	Pr→Cl	Pr→Rw	Rw→Ar	Rw→Cl	Rw→Pr	Avg.
UDA	ResNet-50 [11]	41.1	65.9	73.7	53.1	60.1	63.3	52.2	36.7	71.8	64.8	42.6	75.2	58.4
	MCD [32]	51.7	72.2	78.2	63.7	69.5	70.8	61.5	52.8	78.0	74.5	58.4	81.8	67.8
	MDD [52]	56.2	75.4	79.6	63.5	72.1	73.8	62.5	54.8	79.9	73.5	60.9	84.5	69.7
	CDAN [24]	55.2	72.4	77.6	62.0	69.7	70.9	62.4	54.3	80.5	<b>75.5</b>	61.0	83.8	68.8
	TriDA+CDAN	54.7	74.2	79.6	66.8	75.4	76.1	66.4	54.9	82.4	74.4	<b>62.2</b>	84.0	70.9
SFUDA	SFDA [13]	48.4	73.4	76.9	64.3	69.8	71.7	62.7	45.3	76.6	69.8	50.5	79.0	65.7
	A <sup>2</sup> Net [42]	58.4	79.0	82.4	67.5	79.3	78.9	68.0	56.2	82.9	74.1	60.5	85.0	72.8
	NRC [47]	57.7	<b>80.3</b>	82.0	68.1	79.8	78.6	65.3	56.4	83.0	71.0	58.6	<b>85.6</b>	72.2
	DIPE [39]	56.5	79.2	80.7	<b>70.1</b>	79.8	78.8	67.9	55.1	<b>83.5</b>	74.1	59.3	84.8	72.5
	AaD [49]	<u>59.3</u>	79.3	82.1	68.9	79.8	79.5	67.2	<b>57.4</b>	83.1	72.1	58.5	85.4	72.7
	SFDA-DE [5]	<b>59.7</b>	<u>79.5</u>	<u>82.4</u>	69.7	78.6	79.2	66.1	<u>57.2</u>	82.6	73.9	60.8	85.5	<u>72.9</u>
	DaC [53]	59.1	<u>79.5</u>	81.2	69.3	78.9	79.2	67.4	56.4	82.4	74.0	<u>61.4</u>	84.4	72.8
	SHOT [20]	57.1	78.1	81.5	68.0	78.2	78.1	67.4	54.9	82.2	73.3	58.8	84.3	71.8
	TriDA+SHOT	57.0	77.6	<b>83.0</b>	69.8	81.4	<u>80.7</u>	<b>69.4</b>	53.6	82.9	<u>74.6</u>	59.6	84.6	72.9
	CoWA [17]	56.9	78.4	81.0	69.1	80.0	79.9	67.7	<u>57.2</u>	82.4	72.8	60.5	84.5	72.5
	TriDA+CoWA	58.7	77.7	82.2	69.6	<b>82.0</b>	<b>81.7</b>	<u>69.3</u>	56.2	<b>83.7</b>	73.8	60.5	84.9	<b>73.4</b>

Table 5: Classification accuracy (%) on VisDA-C (ResNet101).

Task	Method	plane	bike	bus	car	horse	knife	mcycle	person	plant	sktbrd	train	truck	Avg.
UDA	ResNet-101 [11]	63.6	35.3	50.6	<u>78.2</u>	74.6	18.7	82.1	16.0	84.2	35.5	77.4	4.7	51.7
	MCD [32]	87.8	75.7	84.2	78.1	91.6	95.3	88.1	78.3	83.4	64.5	84.8	20.9	77.7
	MDD [52]	88.3	62.8	85.2	69.9	91.9	95.1	<b>94.4</b>	81.2	93.8	89.8	84.1	47.9	82.0
	CDAN [24]	94.0	69.2	78.9	57.0	89.8	94.9	91.9	80.3	86.8	84.9	85.0	48.5	80.1
	TriDA+CDAN	95.7	77.3	82.8	58.2	94.2	<b>98.5</b>	93.5	78.0	92.2	90.9	89.7	45.1	83.0
SFUDA	SFDA [13]	86.9	81.7	84.6	63.9	93.1	91.4	86.6	71.9	84.5	58.2	74.5	42.7	76.7
	A <sup>2</sup> Net [42]	94.0	87.8	85.6	66.8	93.7	95.1	85.8	81.2	91.6	88.2	86.5	56.0	84.3
	NRC [47]	<u>96.8</u>	<b>91.3</b>	82.4	62.4	96.2	95.9	86.1	80.6	94.8	94.1	<u>90.4</u>	59.7	85.9
	HCL [12]	93.3	85.4	80.7	68.5	91.0	88.1	86.0	78.6	86.6	88.8	80.0	<b>74.7</b>	83.5
	DIPE [39]	95.2	87.6	78.8	55.9	93.9	95.0	84.1	81.7	92.1	88.9	85.4	58.0	83.1
	AaD [49]	<b>97.4</b>	90.5	80.8	76.2	<b>97.3</b>	96.1	89.8	82.9	95.5	93.0	<b>92.0</b>	<u>64.7</u>	<u>88.0</u>
	SFDA-DE [5]	95.3	<u>91.2</u>	77.5	72.1	95.7	<u>97.8</u>	85.5	<u>86.1</u>	95.5	93.0	86.3	61.6	86.5
	DaC [53]	96.6	86.8	<b>86.4</b>	<b>78.4</b>	96.4	96.2	<u>93.6</u>	83.8	<b>96.8</b>	<b>95.1</b>	89.6	50.0	87.3
	SHOT [20]	94.3	88.5	80.1	57.3	93.1	94.9	80.7	80.3	91.5	89.1	86.3	58.2	82.9
	TriDA+SHOT	96.2	88.7	78.3	53.2	94.5	95.7	80.3	81.2	93.0	89.3	87.1	62.2	83.3
	CoWA [17]	96.2	89.7	83.9	73.8	96.4	97.4	89.3	<b>86.8</b>	94.6	92.1	88.7	53.8	86.9
TriDA+CoWA	96.7	90.6	<u>86.2</u>	<u>77.2</u>	<u>96.7</u>	97.2	92.0	82.6	<u>96.0</u>	<u>94.7</u>	88.6	61.2	<b>88.3</b>	

5.3 Analysis

**Ablation study.** We conduct the ablation study of SFUDA on Office-Home to verify the effect of components in TriDA, including pre-train loss  $\mathcal{L}_I$ , mix loss  $\mathcal{L}_{mix}$  and regularization loss  $\mathcal{L}_{reg}$ . The results are in Table 2. We observe that each component gains performance improvement, and only utilizing  $\mathcal{L}_{mix}$  makes the most contributions (over 0.9% points). In addition, removing  $\mathcal{L}_{reg}$  and  $\mathcal{L}_I$  degrades the accuracy to 72.8%, which verified their effectiveness.

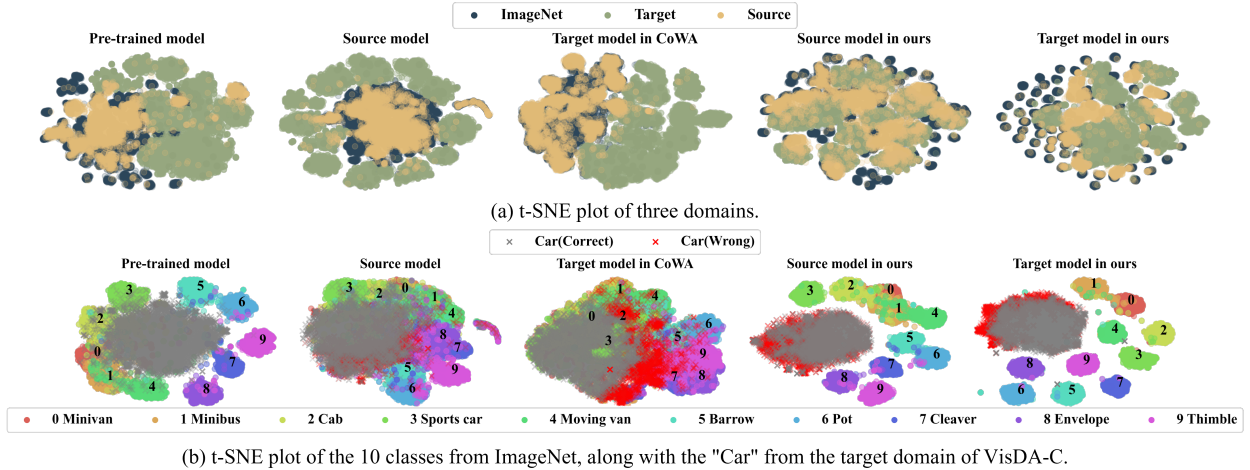


Figure 4: (a)Our method maintains the semantic structures of ImageNet and achieves better alignment between the source and target domain. (b)Incorrect predictions primarily lie on the boundary of unrelated classes in ImageNet. Our method mitigates it by preserving the cluster structure



**Class selection in the pre-train dataset.** We evaluate the number of selected pre-train dataset classes by adjusting the class similarity threshold,  $\tau$ . Table 3 illustrates SFUDA performance on the Office-Home dataset as  $\tau$  ranges from 0.0 to 0.4. The results indicate that selecting merely 63 categories can significantly enhance performance. And a suitable reduction in  $\tau$  further boosts the performance. Additionally, we conduct experiments employing different selection strategies:  $\tau = 0$  (the selection of all), and random selection. The suboptimal performances indicate that selecting semantically irrelevant images aggravates the imbalance issue yet brings less transferable knowledge. More results are shown in the supplementary.

**Visualization.** To demonstrate the limitations of existing methods and the efficacy of our model, we first depict t-SNE [37] of three domains in Figure 4(a). It shows that our method effectively maintains the semantic structures of ImageNet and achieves better alignment between the source and target domain. In Figure 4(b), we illustrate a more specific example, "Car" class from the VisDA-C. Firstly, target samples (in grey and red) are close to ImageNet samples due to semantic similarity. For instance, "Car" is closer to "Minivan" and "Minibus". However, in the adaptation process, ImageNet's cluster structures in the baseline (source model and target model in CoWA) are impaired. These disrupted structures tend to align with target features due to the SP Effect, thereby increasing the risk of adaptation. It also shows that incorrect predictions (red points) primarily lie on the boundary of unrelated classes (red cross near "Cleave" in Figure 4(b)). In contrast, our method mitigates the risks by preserving the cluster structure of ImageNet.

**Incorporating pre-train data.** Firstly, it seems a fair comparison in that existing methods directly use the initialized model pre-trained on a dataset *while* we select its subset without using any new data. Secondly, we use the public dataset free for non-commercial applications, which guarantees accessibility. Finally, our experiments in Section 5.3 demonstrate that incorporating only a minor subset of ImageNet can significantly boost the performance.

## 6 Conclusion

This paper provides a comprehensive study of the pre-train dataset (e.g. ImageNet) in UDA through both empirical and theoretical analysis. We observe the SP effects in UDA and theoretically illustrate that the target risk is bound by gradient disparities of the three domains. Inspired by the above, the proposed TriDA is designed and demonstrated to preserve the pre-train data cluster structure and to outperform the UDA/SFUDA SOTA results.

**Limitations.** A limitation of TriDA is its reliance on the semantic similarity between the pre-train dataset and the target domain. When the target domain significantly deviates from the pre-train one, the performance needs further investigation.

**Broader Impact.** The proposed method improves the UDA performance and the generalization of object classification systems. The societal impact of our work depends upon its application. We generally anticipate a positive broader impact.

## References

- [1] Shekoofeh Azizi, Basil Mustafa, Fiona Ryan, Zachary Beaver, Jan Freyberg, Jonathan Deaton, Aaron Loh, Alan Karthikesalingam, Simon Kornblith, Ting Chen, et al. Big self-supervised models advance medical image classification. In *Proceedings of the IEEE/CVF International Conference on Computer Vision*, pages 3478–3488, 2021.
- [2] Shai Ben-David, John Blitzer, Koby Crammer, Alex Kulesza, Fernando Pereira, and Jennifer Wortman Vaughan. A theory of learning from different domains. *Machine learning*, 79:151–175, 2010.
- [3] Qingchao Chen, Yang Liu, Zhaowen Wang, Ian Wassell, and Kevin Chetty. Re-weighted adversarial adaptation network for unsupervised domain adaptation. In *Proceedings of the IEEE Conference on Computer Vision and Pattern Recognition (CVPR)*, June 2018.
- [4] Jia Deng, Wei Dong, Richard Socher, Li-Jia Li, Kai Li, and Li Fei-Fei. Imagenet: A large-scale hierarchical image database. In *2009 IEEE conference on computer vision and pattern recognition*, pages 248–255. Ieee, 2009.
- [5] Ning Ding, Yixing Xu, Yehui Tang, Chao Xu, Yunhe Wang, and Dacheng Tao. Source-free domain adaptation via distribution estimation. In *Proceedings of the IEEE/CVF Conference on Computer Vision and Pattern Recognition*, pages 7212–7222, 2022.
- [6] Yaroslav Ganin and Victor Lempitsky. Unsupervised domain adaptation by backpropagation. In *International conference on machine learning*, pages 1180–1189. PMLR, 2015.
- [7] Ian Goodfellow, Jean Pouget-Abadie, Mehdi Mirza, Bing Xu, David Warde-Farley, Sherjil Ozair, Aaron Courville, and Yoshua Bengio. Generative adversarial nets. *NeurIPS*, 27, 2014.
- [8] Ishaan Gulrajani and David Lopez-Paz. In search of lost domain generalization. In *International Conference on Learning Representations*, 2020.

- [9] Kaiming He, Ross Girshick, and Piotr Dollar. Rethinking imagenet pre-training. In *Proceedings of the IEEE/CVF International Conference on Computer Vision (ICCV)*, October 2019.
- [10] Kaiming He, Ross Girshick, and Piotr Dollár. Rethinking imagenet pre-training. In *Proceedings of the IEEE/CVF International Conference on Computer Vision*, pages 4918–4927, 2019.
- [11] Kaiming He, Xiangyu Zhang, Shaoqing Ren, and Jian Sun. Deep residual learning for image recognition. In *Proceedings of the IEEE conference on computer vision and pattern recognition*, pages 770–778, 2016.
- [12] Jiaxing Huang, Dayan Guan, Aoran Xiao, and Shijian Lu. Model adaptation: Historical contrastive learning for unsupervised domain adaptation without source data. *Advances in Neural Information Processing Systems*, 34:3635–3649, 2021.
- [13] Youngeun Kim, Donghyeon Cho, Kyeongtak Han, Priyadarshini Panda, and Sungeun Hong. Domain adaptation without source data. *IEEE Transactions on Artificial Intelligence*, 2(6):508–518, 2021.
- [14] Seita Kono, Takaya Ueda, Enrique Arriaga-Varela, and Ikuko Nishikawa. Wasserstein distance-based domain adaptation and its application to road segmentation. In *2021 International Joint Conference on Neural Networks (IJCNN)*, pages 1–7. IEEE, 2021.
- [15] Simon Kornblith, Jonathon Shlens, and Quoc V Le. Do better imagenet models transfer better? In *Proceedings of the IEEE/CVF conference on computer vision and pattern recognition*, pages 2661–2671, 2019.
- [16] Jogendra Nath Kundu, Akshay R Kulkarni, Suvaansh Bhambri, Deepesh Mehta, Shreyas Anand Kulkarni, Varun Jampani, and Venkatesh Babu Radhakrishnan. Balancing discriminability and transferability for source-free domain adaptation. In *International Conference on Machine Learning*, pages 11710–11728. PMLR, 2022.
- [17] Jonghyun Lee, Dahuin Jung, Junho Yim, and Sungroh Yoon. Confidence score for source-free unsupervised domain adaptation. In *International Conference on Machine Learning*, pages 12365–12377. PMLR, 2022.
- [18] Shuang Li, Fangrui Lv, Binhui Xie, Chi Harold Liu, Jian Liang, and Chen Qin. Bi-classifier determinacy maximization for unsupervised domain adaptation. In *AAAI*, 2021.
- [19] Xiangtai Li, Wenwei Zhang, Jiangmiao Pang, Kai Chen, Guangliang Cheng, Yunhai Tong, and Chen Change Loy. Video k-net: A simple, strong, and unified baseline for video segmentation. In *Proceedings of the IEEE/CVF International Conference on Computer Vision*, pages 18847–18857, 2022.
- [20] Jian Liang, Dapeng Hu, and Jiashi Feng. Do we really need to access the source data? source hypothesis transfer for unsupervised domain adaptation. In *International Conference on Machine Learning*, pages 6028–6039. PMLR, 2020.
- [21] Jian Liang, Dapeng Hu, and Jiashi Feng. Domain adaptation with auxiliary target domain-oriented classifier. In *CVPR*, pages 16632–16642, 2021.
- [22] Hongbin Lin, Yifan Zhang, Zhen Qiu, Shuaicheng Niu, Chuang Gan, Yanxia Liu, and Minghui Tan. Prototype-guided continual adaptation for class-incremental unsupervised domain adaptation. In *European Conference on Computer Vision*, 2022.
- [23] Ziquan Liu, Yi Xu, Yuanhong Xu, Qi Qian, Hao Li, Xiangyang Ji, Antoni Chan, and Rong Jin. Improved fine-tuning by better leveraging pre-training data. *Advances in Neural Information Processing Systems*, 35:32568–32581, 2022.
- [24] Mingsheng Long, Zhangjie Cao, Jianmin Wang, and Michael I Jordan. Conditional adversarial domain adaptation. *Advances in neural information processing systems*, 31, 2018.
- [25] George A Miller. *WordNet: An electronic lexical database*. MIT press, 1998.
- [26] Jaemin Na, Heechul Jung, Hyung Jin Chang, and Wonjun Hwang. Fixbi: Bridging domain spaces for unsupervised domain adaptation. In *Proceedings of the IEEE/CVF Conference on Computer Vision and Pattern Recognition*, pages 1094–1103, 2021.
- [27] Duy-Kien Nguyen, Jihong Ju, Olaf Booij, Martin R Oswald, and Cees GM Snoek. Boxer: Box-attention for 2d and 3d transformers. In *Proceedings of the IEEE/CVF International Conference on Computer Vision*, pages 4773–4782, 2022.
- [28] Jiangbo Pei, Zhuqing Jiang, Aidong Men, Liang Chen, Yang Liu, and Qingchao Chen. Uncertainty-induced transferability representation for source-free unsupervised domain adaptation. *IEEE Transactions on Image Processing*, 2023.
- [29] Xingchao Peng, Ben Usman, Neela Kaushik, Judy Hoffman, Dequan Wang, and Kate Saenko. Visda: The visual domain adaptation challenge. *arXiv preprint arXiv:1710.06924*, 2017.

- [30] Maithra Raghu, Chiyuan Zhang, Jon Kleinberg, and Samy Bengio. Transfusion: Understanding transfer learning for medical imaging. *Advances in neural information processing systems*, 32, 2019.
- [31] Kate Saenko, Brian Kulis, Mario Fritz, and Trevor Darrell. Adapting visual category models to new domains. In *Computer Vision—ECCV 2010: 11th European Conference on Computer Vision, Heraklion, Crete, Greece, September 5–11, 2010, Proceedings, Part IV 11*, pages 213–226. Springer, 2010.
- [32] Kuniaki Saito, Kohei Watanabe, Yoshitaka Ushiku, and Tatsuya Harada. Maximum classifier discrepancy for unsupervised domain adaptation. In *CVPR*, pages 3723–3732, 2018.
- [33] Jian Shen, Yanru Qu, Weinan Zhang, and Yong Yu. Wasserstein distance guided representation learning for domain adaptation. In *Proceedings of the AAAI Conference on Artificial Intelligence*, 2018.
- [34] Ilya O Tolstikhin, Bharath K Sriperumbudur, and Bernhard Schölkopf. Minimax estimation of maximum mean discrepancy with radial kernels. *NeurIPS*, 29:1930–1938, 2016.
- [35] Antonio Torralba and Alexei A Efros. Unbiased look at dataset bias. In *2011 IEEE conference on computer vision and pattern recognition*, pages 1521–1528. IEEE, 2011.
- [36] Nilesh Tripuraneni, Michael Jordan, and Chi Jin. On the theory of transfer learning: The importance of task diversity. *Advances in neural information processing systems*, 33:7852–7862, 2020.
- [37] Laurens Van der Maaten and Geoffrey Hinton. Visualizing data using t-sne. *Journal of machine learning research*, 9(11), 2008.
- [38] Hemanth Venkateswara, Jose Eusebio, Shayok Chakraborty, and Sethuraman Panchanathan. Deep hashing network for unsupervised domain adaptation. In *Proceedings of the IEEE conference on computer vision and pattern recognition*, pages 5018–5027, 2017.
- [39] Fan Wang, Zhongyi Han, Yongshun Gong, and Yilong Yin. Exploring domain-invariant parameters for source free domain adaptation. In *Proceedings of the IEEE/CVF Conference on Computer Vision and Pattern Recognition*, pages 7151–7160, 2022.
- [40] Mitchell Wortsman, Gabriel Ilharco, Jong Wook Kim, Mike Li, Simon Kornblith, Rebecca Roelofs, Raphael Gontijo Lopes, Hannaneh Hajishirzi, Ali Farhadi, Hongseok Namkoong, et al. Robust fine-tuning of zero-shot models. In *Proceedings of the IEEE/CVF Conference on Computer Vision and Pattern Recognition*, pages 7959–7971, 2022.
- [41] Yuan Wu, Diana Inkpen, and Ahmed El-Roby. Dual mixup regularized learning for adversarial domain adaptation. In *Computer Vision—ECCV 2020: 16th European Conference, Glasgow, UK, August 23–28, 2020, Proceedings, Part XXIX 16*, pages 540–555. Springer, 2020.
- [42] Haifeng Xia, Handong Zhao, and Zhengming Ding. Adaptive adversarial network for source-free domain adaptation. In *Proceedings of the IEEE/CVF international conference on computer vision*, pages 9010–9019, 2021.
- [43] Ni Xiao and Lei Zhang. Dynamic weighted learning for unsupervised domain adaptation. In *Proceedings of the IEEE/CVF conference on computer vision and pattern recognition*, pages 15242–15251, 2021.
- [44] LI Xuhong, Yves Grandvalet, and Franck Davoine. Explicit inductive bias for transfer learning with convolutional networks. In *International Conference on Machine Learning*, pages 2825–2834. PMLR, 2018.
- [45] Charig Yang, Weidi Xie, and Andrew Zisserman. It’s about time: Analog clock reading in the wild. In *Proceedings of the IEEE/CVF International Conference on Computer Vision*, pages 2508–2517, 2022.
- [46] Luyu Yang, Yan Wang, Mingfei Gao, Abhinav Shrivastava, Kilian Q Weinberger, Wei-Lun Chao, and Ser-Nam Lim. Deep co-training with task decomposition for semi-supervised domain adaptation. In *Proceedings of the IEEE/CVF International Conference on Computer Vision*, pages 8906–8916, 2021.
- [47] Shiqi Yang, Joost van de Weijer, Luis Herranz, Shangling Jui, et al. Exploiting the intrinsic neighborhood structure for source-free domain adaptation. *Advances in neural information processing systems*, 34:29393–29405, 2021.
- [48] Shiqi Yang, Yaxing Wang, Joost Van De Weijer, Luis Herranz, and Shangling Jui. Generalized source-free domain adaptation. In *Proceedings of the IEEE/CVF International Conference on Computer Vision*, pages 8978–8987, 2021.
- [49] Shiqi Yang, Yaxing Wang, Kai Wang, Shangling Jui, et al. Attracting and dispersing: A simple approach for source-free domain adaptation. In *Advances in Neural Information Processing Systems*, 2022.
- [50] Kaichao You, Zhi Kou, Mingsheng Long, and Jianmin Wang. Co-tuning for transfer learning. *Advances in Neural Information Processing Systems*, 33:17236–17246, 2020.

- [51] Hongyi Zhang, Moustapha Cisse, Yann N. Dauphin, and David Lopez-Paz. mixup: Beyond empirical risk minimization. *International Conference on Learning Representations*, 2018.
- [52] Yuchen Zhang, Tianle Liu, Mingsheng Long, and Michael Jordan. Bridging theory and algorithm for domain adaptation. In *International conference on machine learning*, pages 7404–7413. PMLR, 2019.
- [53] Ziyi Zhang, Weikai Chen, Hui Cheng, Zhen Li, Siyuan Li, Liang Lin, and Guanbin Li. Divide and contrast: Source-free domain adaptation via adaptive contrastive learning. *arXiv preprint arXiv:2211.06612*, 2022.